nature biotechnology

Single-base resolution methylomes of tomato fruit development reveal epigenome modifications associated with ripening

Silin Zhong[1,2,5], Zhangjun Fei[1,3,5], Yun-Ru Chen[1], Yi Zheng[1], Mingyun Huang[1], Julia Vrebalov[1], Ryan McQuinn[1], Nigel Gapper[1], Bao Liu[2], Jenny Xiang[4], Ying Shao[4] & James J Giovannoni[1,3]

Ripening of tomato fruits is triggered by the plant hormone ethylene, but its effect is restricted by an unknown developmental cue to mature fruits containing viable seeds. To determine whether this cue involves epigenetic remodeling, we expose tomatoes to the methyltransferase inhibitor 5-azacytidine and find that they ripen prematurely. We performed whole-genome bisulfite sequencing on fruit in four stages of development, from immature to ripe. We identified 52,095 differentially methylated regions (representing 1% of the genome) in the 90% of the genome covered by our analysis. Furthermore, binding sites for RIN, one of the main ripening transcription factors, are frequently localized in the demethylated regions of the promoters of numerous ripening genes, and binding occurs in concert with demethylation. Our data show that the epigenome is not static during development and may have been selected to ensure the fidelity of developmental processes such as ripening. Crop-improvement strategies could benefit by taking into account not only DNA sequence variation among plant lines, but also the information encoded in the epigenome.

Naturally occurring epigenetic changes in a single gene locus in plants can result in heritable morphological variation without alteration of the underlying DNA sequence[1–3]. The model plant *Arabidopsis*, with its compact genome and rapid life cycle, has proven useful in studies of plant epigenetics, including the characterization of DNA methyltransferase enzymes, RNA-directed DNA methylation and transgenerational epigenetic variation during short-term evolution[4–6]. *Arabidopsis* is the first plant for which a whole-genome methylome map was described[7,8]. High-quality reference genomes and improving sequencing technologies have enabled genome analyses of moderate-sized crop genomes, including the recent discovery of hypomethylation in the rice endosperm[9] and the tomato leaf and fruit methylomes reported here. Here we investigate whether global epigenome reprogramming occurs during the economically important process of tomato fruit ripening.

Tomato (*Solanum lycopersicum*) is an important vegetable crop, with a 900-megabase (Mb) genome that has recently been sequenced[10]. It is the primary model plant for studying the development of fleshy fruits, which are differentiated floral tissues that have evolved to aid seed dispersal in angiosperms. Fleshy fruits are unique because they typically undergo a ripening process after seed maturation that involves irreversible changes in color, texture, sugar content, aroma and flavor in order to become succulent and appealing to seed-dispersal vectors (including humans)[8]. Regulation of this process ensures accurate and tissue-specific control of a developmental transition that would be highly detrimental if it were to occur in the wrong tissue or at the wrong stage of fruit maturity.

Ethylene controls the onset of tomato fruit ripening, and reducing its biosynthesis or interfering with its perception inhibits this process[11–14]. However, ethylene is also involved in numerous other aspects of plant growth, development and stress responses, and it cannot induce ripening in immature fruit whose seeds are not viable, which might indicate that additional regulatory constraint(s) affect the transition to ripening competency and the ability to ripen in response to ethylene[11,12]. Although the molecular mechanism of ripening control by ethylene is not fully understood, it is known to be stringent. Applied ethylene can induce ripening early in many fruits, including tomato, but only if they have reached sufficient maturity. In tomato, this stage is associated with the timing of seed maturity—approximately one week before normal ripening, with some variation among cultivars[11]. It is notable that there are no reported genetically engineered or natural mutations that successfully bypass this transition to fruit ethylene-response competence.

RESULTS

Methyltransferase inhibitor induces premature ripening

It has been hypothesized that DNA methylation contributes to the regulation of fruit ripening, because hypermethylation of the gene locus *Cnr* (encoding the transcription factor colorless nonripening) arrests fruit development[3,15]. To test whether changes

[1]Boyce Thompson Institute for Plant Research, Cornell University, Ithaca, New York, USA. [2]Key Laboratories of Molecular Epigenetics of Ministry of Education, Northeast Normal University, Changchun, China. [3]US Department of Agriculture/Agriculture Research Service, Robert W. Holley Centre for Agriculture and Health, Ithaca, New York, USA. [4]Weill Medical College, Genomics Resource Core Facility, Cornell University, New York, New York, USA. [5]These authors contributed equally to this work. Correspondence should be addressed to J.J.G. (jjg33@cornell.edu), Z.F. (zf25@cornell.edu) or S.Z. (sz284@cornell.edu).

Received 1 August 2012; accepted 22 November 2012; published online 27 January 2013; doi:10.1038/nbt.2462

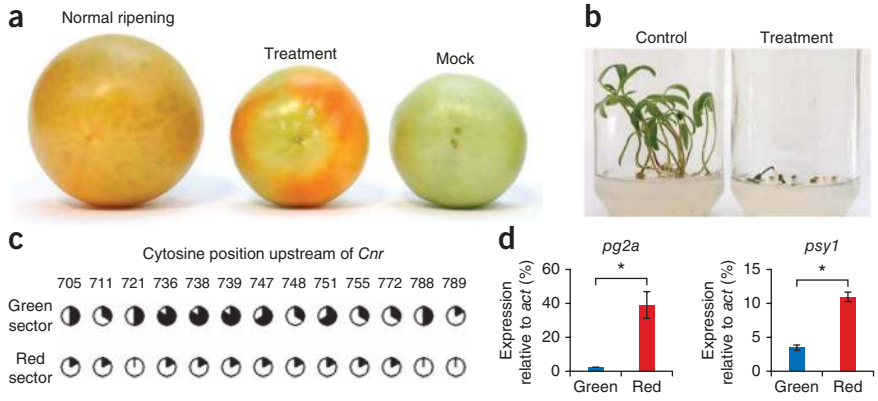

Figure 1 Application of a methylation inhibitor uncouples seed maturation and fruit ripening. (**a**) Tomato fruit (cultivar Ailsa Craig) obtain final size and their seeds become mature at ~39 d.p.a., and ripening begins at ~42 d.p.a. (left, normal ripening). In fruit treated with 5-azacytidine at 17 d.p.a., premature ripening occurred at 30 d.p.a. (center, treatment). The control fruit (right, mock) was treated with water. d.p.a., day post anthesis. (**b**) Seeds isolated from the 5-azacytidine–treated (right, treatment) fruit showing ripening sectors are not viable in the germination assay, whereas seeds isolated from untreated, 42-d.p.a. fruit (left, control) germinate. (**c**) The *Cnr* promoter region was demethylated in the red sectors as determined by Sanger bisulfite sequencing. Numbers indicate the cytosine positions relative to the start of the *Cnr* open reading frame. Black, frequency that the cytosine at the indicated position is methylated. (**d**) Differential expression of known ripening genes between the red and green sectors of 5-azacytidine–treated fruit relative to the normal ripening Ailsa Craig turning (act) fruit **a**. Error bars, s.d. $*P < 0.01$.

in genome methylation might participate in regulation of ripening (and because no methyltransferase mutants are available in tomato), we injected 5-azacytidine, a general inhibitor of DNA (cytosine-5) methyltransferases, into immature tomato fruits and observed early ripening sectors in treated fruit weeks before normal seed maturation (**Fig. 1a**,**b**). Furthermore, bisulfite Sanger sequencing confirmed that the region 5′ upstream of the *Cnr* gene was demethylated in ripening sectors, whereas in green sectors the 5′ upstream region of *Cnr* remained hypermethylated (**Fig. 1c**). We found that the mRNA of hallmark ripening genes—including *pg2a* (encoding the pectinase polygalacturonase) and *psy1*, which encodes phytoene synthase 1, the rate-limiting enzyme in fruit carotenoid synthesis—could be detected in early ripening sectors (**Fig. 1d**). This might indicate that inhibition of DNA cytosine methylation removes the developmental constraint that prevents ripening before seeds are mature, resulting in the uncoupling of the seed-maturation and fruit-development processes.

Sequencing tomato methylomes during fruit development

To further investigate the role of DNA cytosine methylation during the developmental transition from unripe to ripe fruit in loci other than *Cnr*, we used whole-genome bisulfite sequencing[7,8] to profile the methylomes (through detection of 5-methylcytosine modification) of wild-type tomato fruits. Four stages of fruit development were selected, from immature to fully ripe, in addition to ripening-age fruits from two ripening-deficient mutants (carrying *Cnr* and *rin* (ripening inhibitor)) and wild-type leaf tissues. Each methylome was sequenced to >10-fold coverage per strand, and >90% of the genomic cytosine positions were covered (**Supplementary Table 1**). We also annotated the tomato genome for transposable elements and used RNA end sequencing to identify the transcriptional start and termination sites of 17,651 and 18,248 genes, respectively (**Supplementary Tables 2** and **3**), to facilitate more precise characterization of the tomato epigenome. Strand-specific RNA sequencing was then used to profile whole-genome gene expression of each sample, with no fewer than two biological replicates (**Supplementary Tables 4** and **5**).

Tomato is the largest angiosperm and the only fruit whose methylome has been reported to date. More than 60% of its genome consists of heavily methylated transposable elements[10] that are concentrated in the pericentromeric heterochromatin regions (**Fig. 2** and **Supplementary Figs. 1** and **2**). The gene-rich euchromatic regions are located in the chromosome arms and are characterized by reduced methylcytosine density and reduced methylation rates (**Fig. 2b**). In each sample assayed, about half of the genome cytosine positions are methylated, with the majority in the form of asymmetric CHH sites (**Supplementary Fig. 3** and **Supplementary Table 6**), though cytosine methylation context varies locally within genomes and among species. For example, CG is the primary DNA sequence context of cytosine methylation in tomato gene-transcription domains, as in

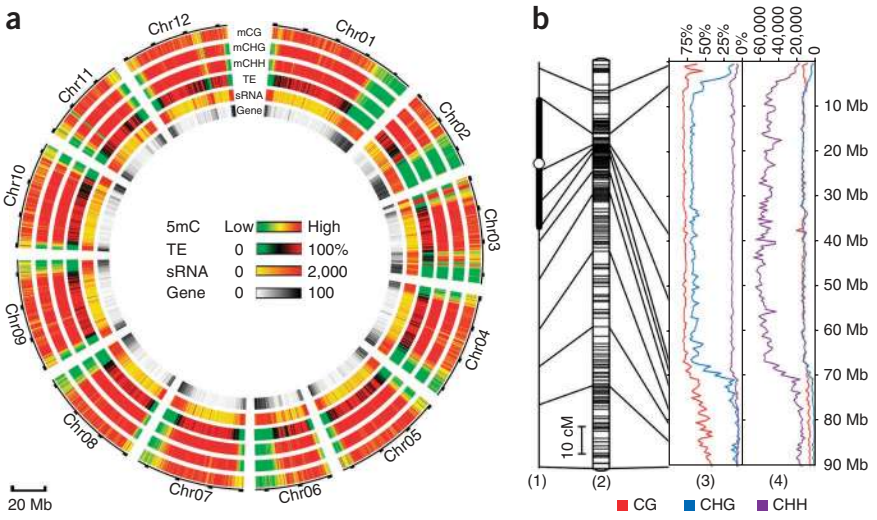

Figure 2 The tomato epigenome. (**a**) Density plot of 5-methylcytosine in sequence contexts (mCG, mCHG, mCHH where mC signifies 5-methylcytosine. H = A, C or T), transposable elements, sRNAs and genes. Chromosome name and scale are indicated on the outer rim. (**b**) Topography of tomato chromosome 1. Horizontal lines indicate the marker positions in each map. (1) Position of the heterochromatin (black rectangle) and centromere (empty circle). (2) Genetic map of tomato chromosome 1 derived from the Kazusa F2-2000 linkage map[10]. (3) DNA methylation rate in each sequence context. (4) Methylcytosine density in each sequence context (bin size, 500 kb). 5mC, 5-methylcytosine; Chr, chromosome; cM, centimorgan; TE, transposable element.

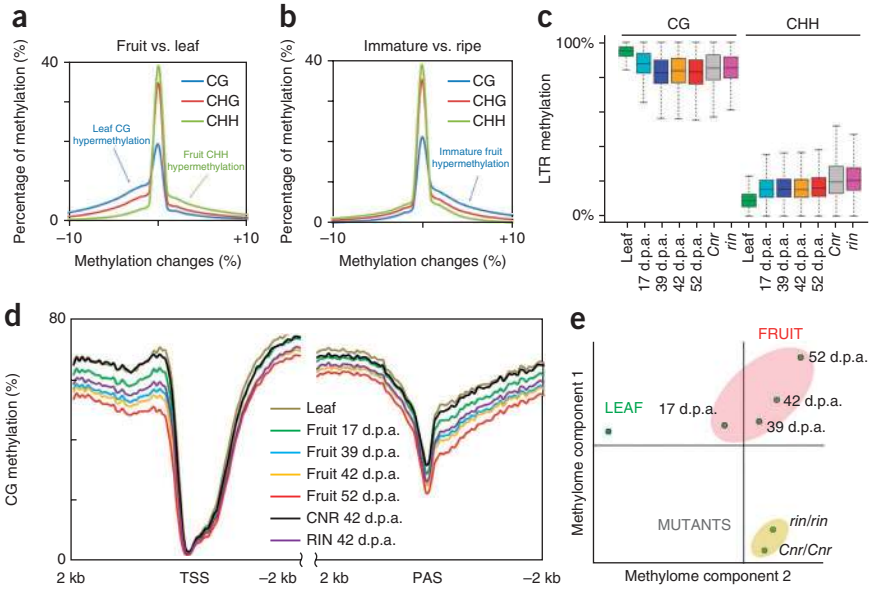

Figure 3 Tissue and developmental specific epigenetic variation in tomato. (**a**,**b**) Frequency of cytosine methylation variation between ripe tomato fruit and leaf (**a**) and immature fruit and ripe fruit (**b**). The *x* axis represents average changes in methylation level between two tissues (bin size, 10 cytosines), and the *y* axis represents the percentage of methylation as defined by cytosine bins showing methylation variation. (**c**) Methylation rate of long terminal repeats (LTRs) in different tissues (as defined in Online Methods). Boxes, quartiles 25–75% black lines within boxes, median of the distribution (quartile 50%). Error bars, quartiles 1–25% (below) and 75–100% (above). (**d**) Change in CG methylation rate in genic regions (bin size, 100 bp). TSS, transcriptional start site; PAS, polyadenylation site. (**e**) Principle component analysis of tomato methylomes of wild-type leaf, wild-type fruits at four developmental stages (17, 39, 42 and 52 d.p.a.) and nonripening mutant fruits at 42 d.p.a.

other eukaryotes. The 5′ regions of genes in both the tomato and rice epigenomes have high levels of CHH methylation associated with miniature inverted transposable elements and 24-nucleotide (nt) small RNA (sRNA)[9], but the 5′ regions of tomato genes have more CG and CHG methylation than their rice counterparts. **Supplementary Figures 4** and **5** show cytosine methylation context, 24-nt sRNA distribution and repeat distributions in tomato.

Previous high-performance liquid chromatography analysis had indicated that the overall cytosine methylation level (~20%) changes little across wild-type tomato tissues[16], which was confirmed by our bisulfite whole-genome sequencing data. However, with the more precise resolution that is possible using bisulfite sequencing, we were able to detect distinctions between tissue- and development-specific methylomes (**Fig. 3a**,**b**). For example, CG and CHG methylation are higher in leaf (85.51% and 56.15%, respectively) than in fruit (73.97–79.16% and 51.99–53.88%, respectively), but CHH methylation is higher in fruit (13.52–14.20%) than in leaf (8.63%); however, overall methylation levels in the two tissues are similar (22.08–24.66%; **Supplementary Table 7**). In addition, the changes in overall genome methylation levels largely reflect changes in methylation of transposable elements (**Fig. 3c** and **Supplementary Fig. 5**), which might indicate that the global epigenetic profile of a moderate-sized genome such as that of tomato is primarily determined by the abundance of its transposon sequences. In addition, we observed that tissues' DNA methylation patterns can change throughout development, as exemplified by the decline in CG methylation as the fruit matures (**Fig. 3b** and **Supplementary Fig. 6**).

To characterize epigenetic variation during fruit development, we used a sliding-window approach (window size, 100 base pairs (bp); step size, 50 bp) to screen for differentially methylated regions (DMRs) between the four wild-type fruit stages (example shown in **Fig. 4a**). A total of 52,095 DMRs were identified, representing ~1% of the tomato genome, and 42,187 (~0.02%) of the cytosine positions were identified as differentially methylated cytosines (DMCs, see Online Methods). We observed enrichment of DMRs and DMCs in genic regions (**Fig. 4b**) that is similar to the transgenerational methylation variation recently reported in *Arabidopsis* using leaf tissue[5,6]. However, a key distinction is that in *Arabidopsis*, many transgenerational methylation variants were located inside genes, whereas tomato DMRs and DMCs are concentrated in regions 5′ upstream of genes (**Fig. 4c**) and are therefore more likely to be associated with promoter regulatory regions.

Hypomethylation during fruit development

We observed that the average methylation level in the 5′ ends of genes gradually declines during wild-type fruit development but remains high in the fruits of ripening-deficient *Cnr* and *rin* mutants (**Fig. 3d** and **Supplementary Fig. 6**). The *Cnr* allele encodes a loss-of-function epimutation in a *SQUAMOSA* promoter binding protein (SBP) transcription factor[3], and *rin* encodes a truncated MADS-box transcription factor[17]. *Cnr* blocked fruit development, and its CG methylation level was the highest and the most similar to that of the wild-type leaf (**Fig. 3d**). The CG methylation level of *rin* fruit at 42 d after anthesis (d.p.a.; the 'breaker' or early ripening stage in the near-isogeneic line) was between those of the wild-type immature and the mature green fruit stages. Principle component analysis of fruit and leaf methylome profiles confirmed that the four wild-type fruit methylomes cluster together (**Fig. 3e**), whereas both nonripening mutants, which contain higher CG and non-CG methylation levels, were separated from those of the wild-type fruit (low CG methylation) and leaf (low non-CG methylation) tissues. These results support a scenario in which the DNA methylation profile not only changes between tissues, but also shows specific and substantial variations in the same tissue (fruit pericarp) as the fruit progresses through development from unripe with immature seeds to ripe with viable seeds.

To investigate the role of cytosine methylation in the 5′ ends of genes, we first examined the methylation pattern in the *Cnr* gene, which is one of the few clearly defined epi-alleles and whose expression is substantially reduced by hypermethylation[3]. From bisulfite sequencing data for the *Cnr* mutant fruit, we could locate the site of the *Cnr* epi-allele, a hypermethylated region 2.3–2.5 kilobases (kb) upstream of the *Cnr* transcriptional start site that is not methylated in the wild type (**Fig. 4a**, red arrow). In wild-type fruit, we found two DMRs in the 5′ end of *Cnr* at 0.7 kb and 1.9 kb upstream of the transcriptional start site (**Fig. 4a**, blue arrows). Notably, these two DMRs become demethylated during ripening, but remain hypermethylated in fruit of both the *Cnr* and *rin* loss-of-function mutants. Similar DMRs that are demethylated during fruit ripening but not in *rin* or *Cnr* fruit were also detected in the putative promoter regions of other known ripening-associated genes (**Supplementary Tables 8–10**), including *pg2a* and *psy1*. These same genes were transcribed in response to the methyltransferase inhibitor 5-azacytidine in immature fruit (**Fig. 1c**),

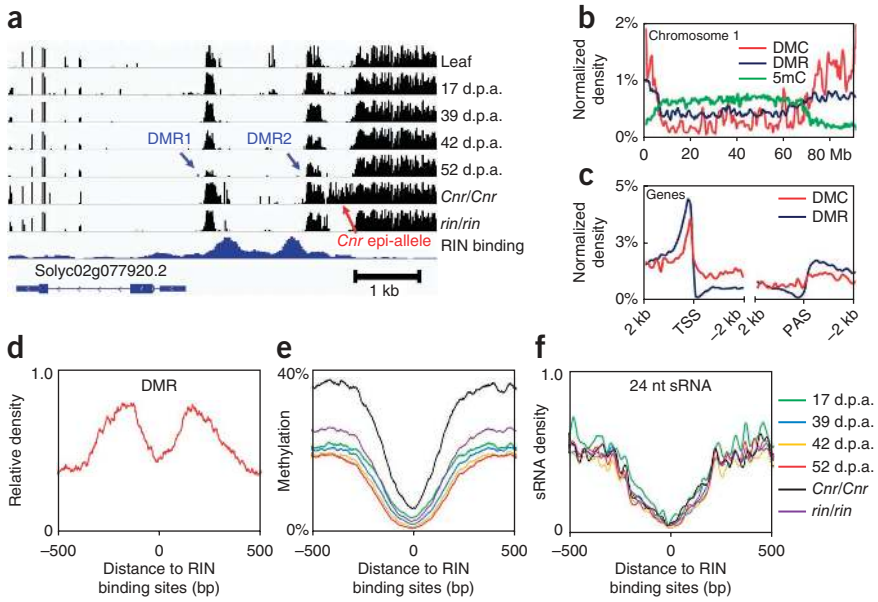

Figure 4 Demethylation of RIN binding sites during ripening. (**a**) DMRs and RIN binding sites in the *Cnr* locus. The locations of DMRs and the *Cnr* epi-allele are indicated by blue and red arrows, respectively. (**b**,**c**) Distribution of DMRs, DMCs and 5-methylcytosines across chromosome 1 (**b**) and gene regions (**c**). (**d**–**f**) Density of DMRs (**d**), average methylation rate (**e**) and 24-nt sRNAs (**f**) near RIN binding sites.

so the DMRs seem to be associated with transcriptional activation by ripening-gene promoters during fruit development.

DMRs and RIN binding in promoters of ripening genes

It has been shown that RIN, a MADS-box transcription factor, directly regulates fruit ripening genes, and its binding is attenuated in the *Cnr* mutant[18]. Analysis of the bisulfite genome sequencing data revealed that the regions near the 5′ ends of genes are hypermethylated in the *Cnr* mutant (**Fig. 3d**). To assess the associations between DMRs and the activation of ripening-gene promoters, we sought to more accurately define functional promoters using chromatin immunoprecipitation sequencing (ChIP-seq) with an antibody to RIN. We found that most of the previously described genes with ripening functions[11] have RIN binding sites (**Supplementary Table 9**). On the basis of the presence of RIN binding sites and differential gene-expression patterns in wild-type fruits and fruits from a nearly isogenic line homozygous for the recessive *rin* loss-of-function mutation (**Supplementary Tables 4** and **5**), we identified 292 candidate genes as RIN targets (**Supplementary Table 9**), including all 16 ripening-associated genes previously described as being regulated by RIN[18–20] (**Supplementary Figs. 7** and **8**). Notably, two fruit-specific ethylene biosynthetic genes (encoding ACC synthases ACS2 and 4) are regulated by RIN[14,21], explaining why *rin* fruits fail to produce ethylene at the onset of ripening. RIN also regulates diverse phenotypes, including fruit color, aroma, cell-wall structure and texture activities, through necessary (and, in some cases, rate-limiting) pathway genes such as *psy1*, *lox* family members (encoding lipoxygenase) and *pg2a*, respectively, which also show RIN binding in their promoters.

We examined methylation changes near RIN binding sites (**Fig. 4d**) and found that the average methylation level is lower than in the neighboring regions in all tissues analyzed, including leaf and immature fruit from which the RIN protein is absent (**Fig. 4e**). This observation is in agreement with data from the human methylomes, in which DNA-protein interaction sites are generally hypomethyated[22].

Furthermore, we found that the RIN binding sites are typically adjacent to DMRs (**Fig. 4d** and **Supplementary Fig. 9**) and become demethylated in all cytosine sequence contexts during ripening (**Fig. 4e** and **Supplementary Fig. 10**), though their sRNA density remains unchanged (**Fig. 4f** and **Supplementary Fig. 11**). Previous studies[10,11,17,18] and massively parallel cDNA sequencing (RNA-seq) experiments in the present study (**Supplementary Tables 4** and **5**) indicate that RIN target genes are upregulated during fruit ripening. Hence, transcription negatively correlates with the methylation status of the RIN binding sites, which are demethylated as fruits mature. A similar global hypomethylation process has been reported in the endosperm and pollen of *Arabidopsis* and rice, but mainly in their transposable elements[4,9,23], whereas tomato transposable elements remain consistently methylated in the three fruit methylomes from tissues harboring mature seed examined from the unripe (mature green) to fully ripe stages (**Fig. 3c** and **Supplementary Fig. 5**). Hypomethylation of tomato transposable elements occurs only at CG sites between the immature and mature green fruit stages and is distinct from the demethylation events at the RIN binding sites, which occur progressively and take place at both CG and non-CG sites (**Supplementary Fig. 10**).

To assess the scale and nature of the epigenome reprogramming that occurs during ripening, we performed Gene Ontology term enrichment analysis of genes that are associated with differentially methylated RIN binding sites. Genes involved in ethylene synthesis and signaling (such as *ACS*, *ACO* (ACC oxidase) and those encoding ethylene receptors), in addition to genes responsible for metabolite changes in ripening (including cell-wall degradation, sugar metabolism and carotenoid, flavonoid and aroma volatile synthesis), were highly enriched (**Supplementary Tables 9** and **11**). Genes encoding fruit-specific transcription factors that regulate fruit development and ripening were also found to be associated with demethylated RIN binding sites (**Supplementary Table 10** and **Supplementary Fig. 9**).

Beyond the RIN binding data described here, little has been done to characterize the promoters of most ripening genes at the molecular level. However, in the early 1990s, promoter-deletion studies were used to analyze the ripening genes *E8* and *pg2a*[24,25]. We found DMRs and RIN binding sites in the promoters of both genes—specifically, in regions that disrupt their expression when deleted (**Supplementary Table 10**). A previous report showed that RIN failed to bind these sites in the hypermethylated *Cnr* mutant[18], supporting the assertion that epigenetic changes during normal fruit development may contribute to the regulation of promoter activity. Although we cannot extrapolate on the basis of these data alone that hypomethylation facilitates regulator binding (or vice versa), these observations might indicate that at least some effects on the methylation of necessary ripening genes are influenced directly or indirectly by CNR and RIN activity and that these effects are preceded by other methylation changes, which probably reflect the action of additional developmental regulators that facilitate the epigenome changes heralding later fruit maturation.

On the basis of the observations that (i) ripening-gene promoters were demethylated during wild-type fruit development and became

hypermethylated in ripening-deficient mutants (**Fig. 3d**) and (ii) methylation inhibitor treatment induced early ripening before seed maturation (**Fig. 1a**), and given the lack of RIN binding in the hypermethylated *Cnr* mutant[18], we propose that genome methylation status is one of the key determining factors in the repression of fruit ripening before seed maturation.

DISCUSSION

It has long been hypothesized that a developmental signal is required to transition fruit development toward ripening[11,12,26]. This signal is clearly not systematic and so differs from those involved in vernalization or the autonomous pathway, as plants can bear fruits ranging from very immature to fully ripe at the same time. Nor is this signal likely to be derived from the seed, as parthenocarpic (seedless) fruits ripen completely and in a normal time frame. Examples include banana, table grape and naval orange varieties that are widely used in agriculture, in addition to natural and transgenic tomato parthenocarpic mutants[27,28]. A prevailing model of ripening control, based on physiological observations and experiments, describes two 'systems' of ethylene that determine the competency for ripening initiation: fruit undergoes a developmental transition from ethylene system I (ripening repressive) to ethylene system II (ripening promoting) that enables ripening[11,12,26]. The molecular nature of this two-system model remains largely unknown. Here, we show with whole-genome bisulfite sequencing that substantial global epigenome reprogramming occurs throughout fruit development, and that location-specific epigenetic changes occur in the RIN target promoters during fruit ripening, which is consistent in timing with the unknown constraint over fruit ripening control.

Our observation that RIN binding sites are hypermethylated in the *rin* loss-of-function mutant shows notable similarities with recent findings from the human ENCODE project[29] and a study of the mouse epigenome[30], which showed that promoter methylation status was altered by transcription factor binding. Although the correlation between RIN binding sites and demethylation and the promoter hypermethylation in the *rin* mutant are fully consistent with the results of these mammalian studies, very early ripening with methyltransferase-inhibitor treatment suggests that in the fruit system, chemical-induced demethylation preceding transcription factor binding is enough to influence a developmental process. These two processes may interact such that transcription factor binding and the promoter methylation status balance transcriptional activation. On the basis of our results and previous studies, we propose a three-component model for the control of fruit ripening in which, through interacting mechanisms that remain unclear, the ripening hormone ethylene and fruit-specific transcription factors, together with epigenome reprogramming, transition the fruit into a ripening-competent state when the seeds become viable (**Fig. 5**). Angiosperms seem to use their epigenomic stability as a supplemental regulatory constraint over an irreversible developmental transition that could have severe negative consequences if it were to occur in immature fruit or in non-fruit tissues.

This study provides insights into the potential role of a dynamic epigenome in plant development. In addition, previous searches for the 'missing developmental cue' that promotes ripening and is of significant agricultural value were focused on allelic diversity and hormone signaling. Indeed, plant-breeding programs depend on DNA-based molecular markers and might overlook much epigenetic variation. Hence, our results highlight the importance of establishing future crop-improvement strategies and technologies that consider not only genetic variation, but also epigenetic variation, which, at present, is not part of modern crop breeding and for which simple and economical assays now need to be developed. In the case of fruit ripening and quality, the DMRs associated with ripening, shelf-life and fruit-quality genes described here provide an initial set of targets for analyses of epigenomic variation across germplasm collections and for assessment of variations that may form the basis of future expanded selection strategies. On the basis of our data for tomato, priority candidates include genes that are already selection targets but for which there are few sequence-based, functional polymorphism–limiting breeding outcomes. These genes and additional candidates with known or suspected roles in fruit biology (and, thus, functional potential) are listed in **Supplementary Table 12**. Examples include *rin*, *nor* and *pg2a*, all of which influence shelf life and quality, and *psy1* and *pds*, which affect mature fruit color. A number of additional genes whose expression affects shelf life and quality have been defined in mutant or transgenic plants, with little if any documented functional sequence variation (for example, *Cnr*, *TAGL1*, *HB1*, *nr*, *etr4*, *exp1* and *acs4*). These genes have been minimally (if at all) exploited to date and might also serve as likely candidates for tomato improvement, should epigenetic variants be discovered.

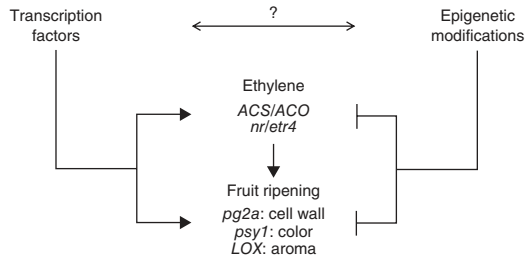

Figure 5 Model of fruit ripening regulation. In nonfruit tissues and immature fruits without viable seeds, ripening does not occur, and promoters of key ripening genes are hypermethylated. In maturing wild-type fruits, these promoters become demethylated by a yet-to-be-identified mechanism that is influenced by the transcription factors RIN and CNR. Whether transcription-factor binding facilitates promoter hypomethylation, hypomethylation facilitates DNA binding or both activities influence the ripening transition remains unclear. This fact is represented in the figure by the double-ended arrow with a question mark. However, it is noteworthy that early promoter demethylation by inhibitor treatment is sufficient to initiate premature ripening. After changes in promoter methylation and transcription factor activity, ripening is initiated with a burst of ethylene production through *ACS* and *ACO* with signaling through ethylene receptors *nr* and *etr4* and the activation of downstream ripening genes, including those regulating cell-wall degradation (*pg2a*), carotenoid synthesis (*psy1*) and aroma volatile production (*LOX*).

METHODS

Methods and any associated references are available in the online version of the paper.

Accession code. NCBI Sequence Read Archive (raw sequence data): SRA046092, SRA046132, SRA046131, SRA053345 and SRA046480. Analyzed data can be accessed from the tomato epigenome database (http://ted.bti.cornell.edu/epigenome/).

Note: Supplementary information is available in the online version of the paper.

ACKNOWLEDGMENTS

We thank E. Richards, R. Schmitz and J. Ecker for discussion and thoughtful advice in preparing this manuscript, and R. White, Y. Xu and Z. Li for technical assistance. This project was supported by the United States Department of Agriculture – Agricultural Research Service, National Science Foundation IOS-0606595 and IOS-0923312 to J.J.G. and Z.F., DBI-0820612 to J.J.G., National Natural Science Foundation of China 30900783 and 3090243 to S.Z. and B.L. and the Human Frontier Science Program LTF000076/2009 to S.Z.

AUTHOR CONTRIBUTIONS

J.J.G., Z.F. and S.Z. devised the project and wrote the manuscript. Z.F. and S.Z. led the bioinformatic and experimental teams, respectively. Y.-R.C., J.V., R.M. and N.G. performed the experiments. Y.Z., Z.F., M.H., B.L., Y.S., J.X. and J.J.G. analyzed and interpreted the data.

COMPETING FINANCIAL INTERESTS

The authors declare no competing financial interests.

Published online at http://www.nature.com/doifinder/10.1038/nbt.2462.
Reprints and permissions information is available online at http://www.nature.com/reprints/index.html.

1. Patterson, G.I., Thorpe, C.J. & Chandler, V.L. Paramutation, an allelic interaction, is associated with a stable and heritable reduction of transcription of the maize *b* regulatory gene. *Genetics* **135**, 881–894 (1993).
2. Cubas, P., Vincent, C. & Coen, E. An epigenetic mutation responsible for natural variation in floral symmetry. *Nature* **401**, 157–161 (1999).
3. Manning, K. *et al.* A naturally occurring epigenetic mutation in a gene encoding an SBP-box transcription factor inhibits tomato fruit ripening. *Nat. Genet.* **38**, 948–952 (2006).
4. Law, J.A. & Jacobsen, S.E. Establishing, maintaining and modifying DNA methylation patterns in plants and animals. *Nat. Rev. Genet.* **11**, 204–220 (2010).
5. Becker, C. *et al.* Spontaneous epigenetic variation in the *Arabidopsis* thaliana methylome. *Nature* **480**, 245–249 (2011).
6. Schmitz, R.J. *et al.* Transgenerational epigenetic instability is a source of novel methylation variants. *Science* **334**, 369–373 (2011).
7. Cokus, S.J. *et al.* Shotgun bisulphite sequencing of the *Arabidopsis* genome reveals DNA methylation patterning. *Nature* **452**, 215–219 (2008).
8. Lister, R. *et al.* Highly integrated single-base resolution maps of the epigenome in *Arabidopsis*. *Cell* **133**, 523–536 (2008).
9. Zemach, A. *et al.* Local DNA hypomethylation activates genes in rice endosperm. *Proc. Natl. Acad. Sci. USA* **107**, 18729–18734 (2010).
10. The Tomato Genome Consortium. The tomato genome sequence provides insights into fleshy fruit evolution. *Nature* **485**, 635–641 (2012).
11. Klee, H.J. & Giovannoni, J.J. Genetics and control of tomato fruit ripening and quality attributes. *Annu. Rev. Genet.* **45**, 41–59 (2011).
12. Burg, S.P. & Burg, E.A. Ethylene action and the ripening of fruits. *Science* **148**, 1190–1196 (1965).
13. Hamilton, A.J., Lycett, G.W. & Grierson, D. Antisense gene that inhibits synthesis of the hormone ethylene in transgenic plants. *Nature* **346**, 284–287 (1990).
14. Oeller, P.W., Lu, M.W., Taylor, L.P., Pike, D.A. & Theologis, A. Reversible inhibition of tomato fruit senescence by antisense RNA. *Science* **254**, 437–439 (1991).
15. Seymour, G., Poole, M., Manning, K. & King, G.J. Genetics and epigenetics of fruit development and ripening. *Curr. Opin. Plant Biol.* **11**, 58–63 (2008).
16. Messeguer, R., Ganal, M.W., Steffens, J.C. & Tanksley, S.D. Characterization of the level, target sites and inheritance of cytosine methylation in tomato nuclear DNA. *Plant Mol. Biol.* **16**, 753–770 (1991).
17. Vrebalov, J. *et al.* A MADS-box gene necessary for fruit ripening at the tomato ripening-inhibitor (*Rin*) locus. *Science* **296**, 343–346 (2002).
18. Martel, C., Vrebalov, J., Tafelmeyer, P. & Giovannoni, J.J. The tomato MADS-box transcription factor ripening inhibitor interacts with promoters involved in numerous ripening processes in a colorless nonripening–dependent manner. *Plant Physiol.* **157**, 1568–1579 (2011).
19. Ito, Y. *et al.* DNA-binding specificity, transcriptional activation potential, and the *rin* mutation effect for the tomato fruit-ripening regulator RIN. *Plant J.* **55**, 212–223 (2008).
20. Fujisawa, M., Nakano, T. & Ito, Y. Identification of potential target genes for the tomato fruit-ripening regulator RIN by chromatin immunoprecipitation. *BMC Plant Biol.* **11**, 26 (2011).
21. Barry, C.S., Llop-Tous, M.I. & Grierson, D. The regulation of 1-aminocyclopropane-1-carboxylic acid synthase gene expression during the transition from system-1 to system-2 ethylene synthesis in tomato. *Plant Physiol.* **123**, 979–986 (2000).
22. Lister, R. *et al.* Human DNA methylomes at base resolution show widespread epigenomic differences. *Nature* **462**, 315–322 (2009).
23. Feng, S., Jacobsen, S.E. & Reik, W. Epigenetic reprogramming in plant and animal development. *Science* **330**, 622–627 (2010).
24. Deikman, J., Kline, R. & Fischer, R.L. Organization of ripening and ethylene regulatory regions in a fruit-specific promoter from tomato (*Lycopersicon esculentum*). *Plant Physiol.* **100**, 2013–2017 (1992).
25. Nicholass, F.J., Smith, C.J., Schuch, W., Bird, C.R. & Grierson, D. High levels of ripening-specific reporter gene expression directed by tomato fruit polygalacturonase gene-flanking regions. *Plant Mol. Biol.* **28**, 423–435 (1995).
26. McMurchie, E.J., McGlasson, W.B. & Eaks, I.L. Treatment of fruit with propylene gives information about the biogenesis of ethylene. *Nature* **237**, 235–236 (1972).
27. King, G.N. Artificial parthenocarpy in *Lycopersicum esculentum*; tissue development. *Plant Physiol.* **22**, 572–581 (1947).
28. Wang, H. *et al.* Regulatory features underlying pollination-dependent and -independent tomato fruit set revealed by transcript and primary metabolite profiling. *Plant Cell* **21**, 1428–1452 (2009).
29. Thurman, R.E. *et al.* The accessible chromatin landscape of the human genome. *Nature* **489**, 75–82 (2012).
30. Stadler, M.B. *et al.* DNA-binding factors shape the mouse methylome at distal regulatory regions. *Nature* **480**, 490–495 (2011).

ONLINE METHODS

Plant materials. Wild-type tomato (*Solanum lycopersicum* cultivar Ailsa Craig) and the corresponding *Cnr* and *rin* loss-of-function mutants were grown under standard greenhouse conditions (12 h supplemental lighting at 26 °C and 12 h at 20 °C). Tomato fruit pericarp tissues were harvested at 17 (immature), 39 (mature green), 42 (breaker/early ripening), and 52 d (red ripe) after anthesis (d.p.a.). Tomato leaf tissues were harvested from 1-month-old wild-type tomato seedlings. For methyltransferase inhibitor treatment, 50 µL of 1 mM 5-azacytidine aqueous solution was injected into the columella of immature fruits from the pedicel and bottom, and the injection was repeated each week. The negative control fruits were injected with water. DNA was isolated separately from the nonripening (green) and ripening (red) sectors on the 5-azacytidine–treated fruits when premature ripening occurred.

Strand-specific RNA sequencing. Strand-specific RNA sequencing libraries were constructed as previously described[31]. For each sample, two to four biological replicates were sequenced. All sequencing reactions were performed on GAIIx or HiSeq2000 according to the manufacturer's instructions in the core facility of Cornell Weill Medical College.

Small RNA sequencing. sRNA sequencing was performed as previously described[32]. Purified sRNA was first ligated to 3′ adaptor by T4 RNA ligase 2 truncated (NEB) in the presence of 20% PEG. The ligation product was separated by urea-PAGE and purified, followed by 5′ adaptor ligation with T4 RNA ligase 1 in the presence of ATP and 20% PEG. The ligation product was RT-PCR amplified before sequencing.

RNA end sequencing. RNA end sequencing was performed to annotate the 5′ and 3′ ends of tomato genes. Poly(A) RNA samples were first dephosphorylated by alkaline phosphatase and their 5′ cap structure was removed by tobacco acid pyrophosphatase. They were then ligated to the Illumina 5′ small RNA adaptor by RNA ligase 1. After fragmentation, the 3′ small RNA adaptor was attached by RNA ligase 2, truncated. The library was then RT-PCR enriched and sequenced. To sequence the 3′ end of genes, poly(A) samples were fragmented and reverse transcribed with oligo-dT(10) VN primer (5′ p-TTTTTTTTTTVN 3′), hence only the junction between the 3′ UTR and the poly(A) tail could be primed. Illumina libraries were constructed as previous described[29].

Chromatin immunoprecipitation sequencing. Ripening fruit tissues (42 d.p.a.) were fixed with 1% formaldehyde for 15 min under vacuum and ground to fine power under liquid nitrogen. Nuclei were isolated as previously described[33]. ChIP was performed using the affinity purified polyclonal antibody against the RIN protein. Illumina ChIP-Seq libraries were constructed using TruSeq index adapters as previous described[31]. Three biological replicates were sequenced.

Genome bisulfite sequencing. Bisulfite sequencing (BS-Seq) was carried out as previously described[8] using a fully methylated Y-shape paired-end adaptor. After two rounds of sodium bisulfite conversion using the EpiTeck Kit (Qiagen), the ligated product was PCR amplified using a uracil-tolerant proofreading enzyme (PfuTurboCx, Stratagene). To achieve no less than 10× genome coverage, 14, 9 and 10 libraries were sequenced on Illumina GAIIx platform for the immature green fruit at 17 d.p.a., ripening fruit at 42 d.p.a. and fully ripe fruit at 52 d.p.a., respectively, and two, three, one and four libraries were sequenced using the HiSeq2000 platform for wild-type tomato leaf tissue, wild-type mature green fruit at 39 d.p.a., *Cnr* mutant fruit at 42 d.p.a. and *rin* mutant fruit at 42 d.p.a., respectively. An *Arabidopsis* leaf BS-Seq library was sequenced in parallel and analyzed as a control (**Supplementary Table 6** and **Supplementary Fig. 3**). Two non-bisulfite–treated tomato genomic DNA libraries were also sequenced as negative controls.

Measurement of methylation level in *Cnr* locus by bisulfite PCR. Genomic DNA was bisulfite converted using the EZ DNA methylation kit (Zymo) and PCR amplified with EpiMark HotStart Taq (NEB) using degenerative primers YYATAGAYYAAAGYYAGTGGTTTGTAGTGAATTG and CCRACATRRACAACTRARA RACCAACTTRCA, which amplify the DMR region in the promoter of *Cnr*. The PCR products were cloned into pGEM-T-Easy vector (Promega) for Sanger sequencing.

RNA-Seq data processing. Strand-specific RNA-Seq reads were first aligned to adaptor, ribosomal RNA and tRNA sequences using Bowtie and allowing two mismatches[34]. The resulting filtered reads were aligned to the tomato genome using Tophat and allowing one segment mismatch[35]. Following alignments, raw counts for each tomato gene were normalized to reads per kilobase of exon model per million mapped reads (RPKM). To identify differentially expression genes during fruit development, the expression data were first transformed using the getVarianceStabilizedData function in the DESeq package[36]. The variance-stabilizing transformed RNA-Seq expression data were then fed to the LIMMA package[37], and F tests were performed. Differentially expressed genes between wild-type and mutant fruits were identified with DESeq. Raw *P* values of multiple tests were corrected using FDR[38]. Genes with FDR <0.01 and RPKM value >10 in at least one of the tissues or fruit stages were defined as differentially expressed genes. For 5′ and 3′ end sequencing, adaptor sequence and poly(T)10 sequences from the 3′RNA-Seq reads were trimmed. To define transcriptional start sites (TSS) and polyadenylation sites (PAS), both 5′ and 3′ reads were aligned to the tomato genome using Bowtie. Reads aligned to multiple locations were discarded. Tomato genome regions containing 5′ or 3′ end reads derived from the sense strand of the corresponding gene models were identified as TSS and PAS, respectively. If multiple TSS or PAS sites were identified for a single gene, the one with the highest read coverage was used.

Small-RNA read processing and alignment. sRNA reads were first identified to contain 3′ adaptor sequences, and only bases preceding the adaptor sequences were kept. The resulting sRNA sequences were further processed to remove those containing base *n* (where *n* is a base that could not be accurately called) or having lengths <15 bp. The remaining high-quality sRNA reads were aligned to the tomato genome using Bowtie with perfect matches. Reads aligned to multiple locations in the tomato genome were not included in the analysis.

Identification of target promoters of the MADS-box transcription factor RIN. ChIP-Seq read alignment was performed using Bowtie[34], and only uniquely aligned reads were retained. RIN binding sites were identified using MACS[39]. To identify candidate RIN targets, we first filtered genes without differential expression pattern between wild-type and *rin* loss-of-function mutant fruits. We further filtered genes without differential expression between immature wild-type fruit (17 d.p.a.), in which *rin* has yet been expressed, and ripening fruits.

Bisulfite-sequencing-read processing and alignment. Reads were first aligned to the plastid genome, which is unmethylated, to calculate the conversion rate. Cytosine bases in the reads were first replaced with thymines, and the resultant reads were then aligned to the two computationally converted strands of the tomato plastid genome (one with C to T and the other with G to A), respectively, using Bowtie with perfect matches[34]. Cytosine conversion rate was then calculated from the alignments by dividing number of converted cytosines by total of number of cytosines. To align the reads to tomato genome sequences, reads from each independent library were processed to remove clonal reads by keeping only one of the identical reads. Cytosine bases in the reads were then replaced with thymines. The converted reads were aligned to the computationally converted strands of the tomato genome (one with C to T and the other with G to A), respectively, using the Bowtie algorithm allowing up to two mismatches. Alignments from both strands were combined, and for each read only the optimal alignments were kept. Multi-aligned reads, which were mapped to the tomato genome at more than one location, were not included in the analysis. The read sequences in the alignments were then replaced with the original, nonconverted sequences. Finally, methylation status of each cytosine in tomato genome was calculated on the basis of the alignments.

Identification of methylated cytosine sites. The binomial test was performed for each cytosine base in the tomato genome to check whether the cytosine site can be called a methylated cytosine site. Three types of potential errors are

doi:10.1038/nbt.2462

present in the BS-Seq data set, namely incomplete bisulfite conversion, nucleotide polymorphisms and sequencing errors. Bisulfite conversion rate was derived from the alignments to the tomato plastid genome. Nucleotide polymorphisms and sequencing errors were calculated as the frequency of mismatched bases in the uniquely aligned reads. For each cytosine site, binomial probability was calculated as $B(x \geq k; n, p)$, where n is the total number of reads covering the site (read depth), k is the total number of the methylated cytosines identified at the site and p is the error rate. The resultant binomial probability can be interpreted as the probability of at least k methylated cytosines obtained from n trials (read depth) owing to the errors in which the error rate is p. Binomial probability values were then adjusted for multiple tests using FDR[38]. Cytosine sites with FDR <0.01 were defined as methylated cytosine sites.

Identification of differentially methylated regions. A sliding-window approach was used to screen regions in the tomato genome that were differentially methylated during fruit development. Only cytosine sites covered by at least four reads were used. A window size of 100 bp, progressing 50 bp per iteration, was used in this analysis. Windows with fewer than 20 sequenced cytosine sites were discarded. For each window, the methylation level at each cytosine site was calculated for each of the four fruit developmental stages. A Kruskal–Wallis test was then performed for each window. *P* values from Kruskal–Wallis tests were corrected for multiple tests with FDR. Windows with FDR <0.05 and changes of methylation level during fruit development of at least two-fold were identified as differentially methylated regions (DMRs). Overlapping DMRs were concatenated.

Identification of differentially methylated cytosines. DMC identification was performed as previously described[7,8] using Fisher's exact test. Only cytosine positions determined to be a methylated cytosine site by the binomial test and covered by at least four reads in at least one fruit developmental stage were used for the analysis. The resulting *P* values were corrected for multiple tests with FDR. Cytosine sites with FDR <0.01 and changes of methylation level of at least two-fold were identified as DMCs.

31. Zhong, S. *et al.* High-throughput illumina strand-specific RNA sequencing library preparation. *Cold Spring Harb. Protoc.* **2011**, 940–949 (2011).
32. Chen, Y.R. *et al.* A cost-effective method for Illumina small RNA-Seq library preparation using T4 RNA ligase 1 adenylated adapters. *Plant Methods* **8**, 41 (2012).
33. Ricardi, M.M., Gonzalez, R.M. & Iusem, N.D. Protocol: fine-tuning of a chromatin immunoprecipitation (ChIP) protocol in tomato. *Plant Methods* **6**, 11 (2010).
34. Langmead, B., Trapnell, C., Pop, M. & Salzberg, S.L. Ultrafast and memory-efficient alignment of short DNA sequences to the human genome. *Genome Biol.* **10**, R25 (2009).
35. Trapnell, C., Pachter, L. & Salzberg, S.L. TopHat: discovering splice junctions with RNA-Seq. *Bioinformatics* **25**, 1105–1111 (2009).
36. Wang, L.K., Feng, Z.X., Wang, X., Wang, X.W. & Zhang, X.G. DEGseq: an R package for identifying differentially expressed genes from RNA-seq data. *Bioinformatics* **26**, 136–138 (2010).
37. Smyth, G.K. Linear models and empirical bayes methods for assessing differential expression in microarray experiments. *Stat. Appl. Genet. Mol. Biol.* **3**, 3 (2004).
38. Benjamini, Y. & Hochberg, Y. Controlling the false discovery rate—a practical and powerful approach to multiple testing. *J. R. Stat. Soc., B* **57**, 289–300 (1995).
39. Zhang, Y. *et al.* Model-based analysis of ChIP-Seq (MACS). *Genome Biol.* **9**, R137 (2008).

Epigenetic control of tomato fruit development

Silin Zhong[1,2*,†], Zhangjun Fei[1,3,*,†], Yun-Ru Chen[1], Yi Zheng[1], Mingyun Huang[1], Julia Vrebalov[1], Ryan McQuinn[1], Nigel Gapper[1], Bao Liu[2], Jenny Xiang[4], Ying Shao[4], James J. Giovannoni[1,3*]

[1]Boyce Thompson Institute for Plant Research, Cornell University, USA

[2] Key Laboratories of Molecular Epigenetics of MOE, Northeast Normal University, Changchun, China

[3]U.S. Department of Agriculture/Agriculture Research Service, Robert W. Holley Centre for Agriculture and Health, USA

[4]Weill Medical College, Cornell University, USA

* To whom correspondence should be addressed: James Giovannoni (jjg33@cornell.edu), Zhangjun Fei (zf25@cornell.edu), Silin Zhong (sz284@cornell.edu)

†Equal contribution

Supplementary Figures S1 to S11

All data presented in this study can be assessed from the Tomato Epigenome Database (http://ted.bti.cornell.edu/epigenome)

Nature Biotechnology: doi:10.1038/nbt.2462

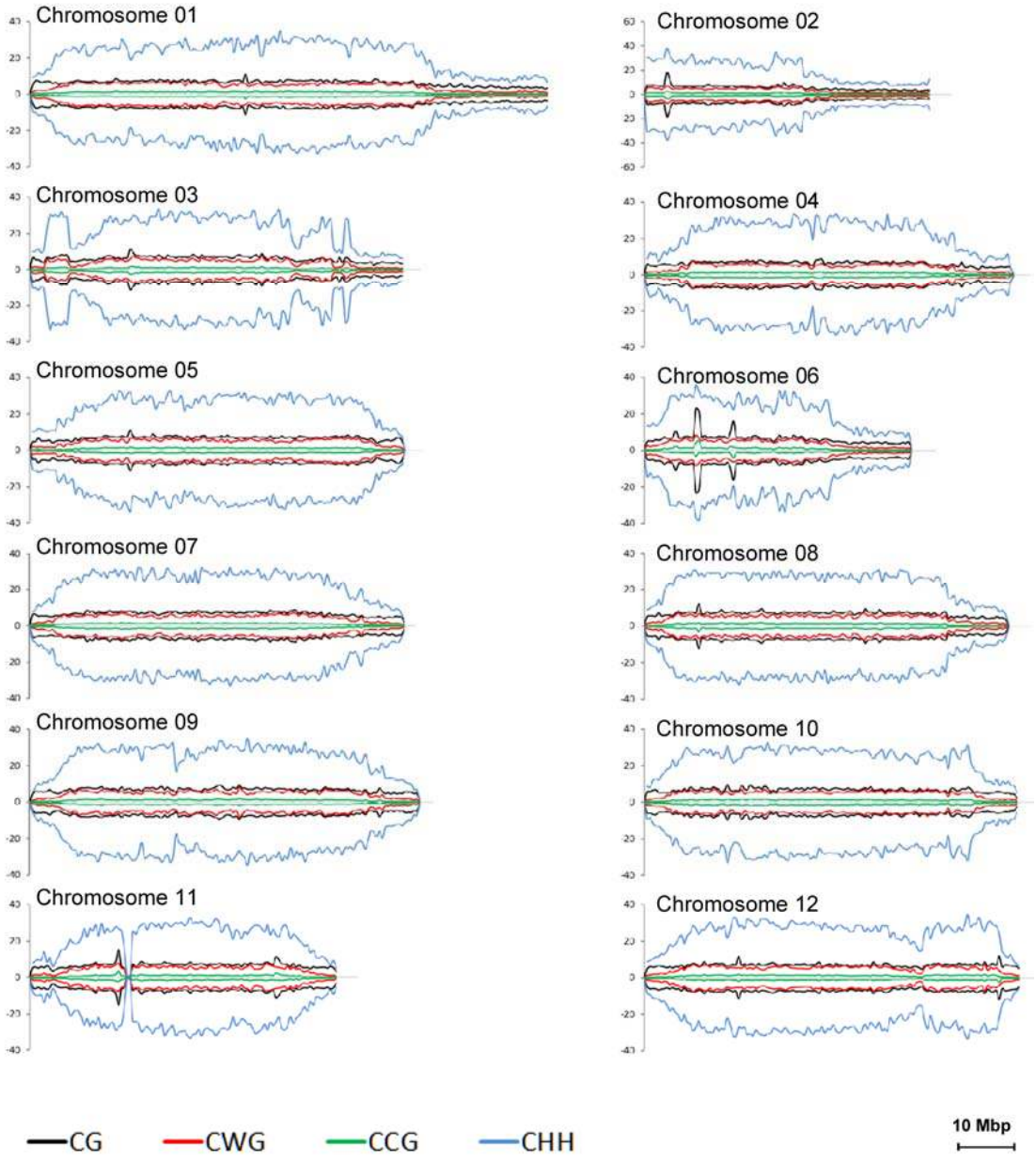

Supplementary Figure 1 | Density plot of 5-methylcytosine in the 12 tomato chromosomes of mature green fruit for each of four methylated cytosine sequence contexts. Y-axis indicates the number (in 1000's) of 5mC in each 500 kb chromosome window. The area above zero refers to cytosines residing in the Crick strand and that below refers to the Watson strand. Line color reflects the indicated cytosine sequence context.

Nature Biotechnology: doi:10.1038/nbt.2462

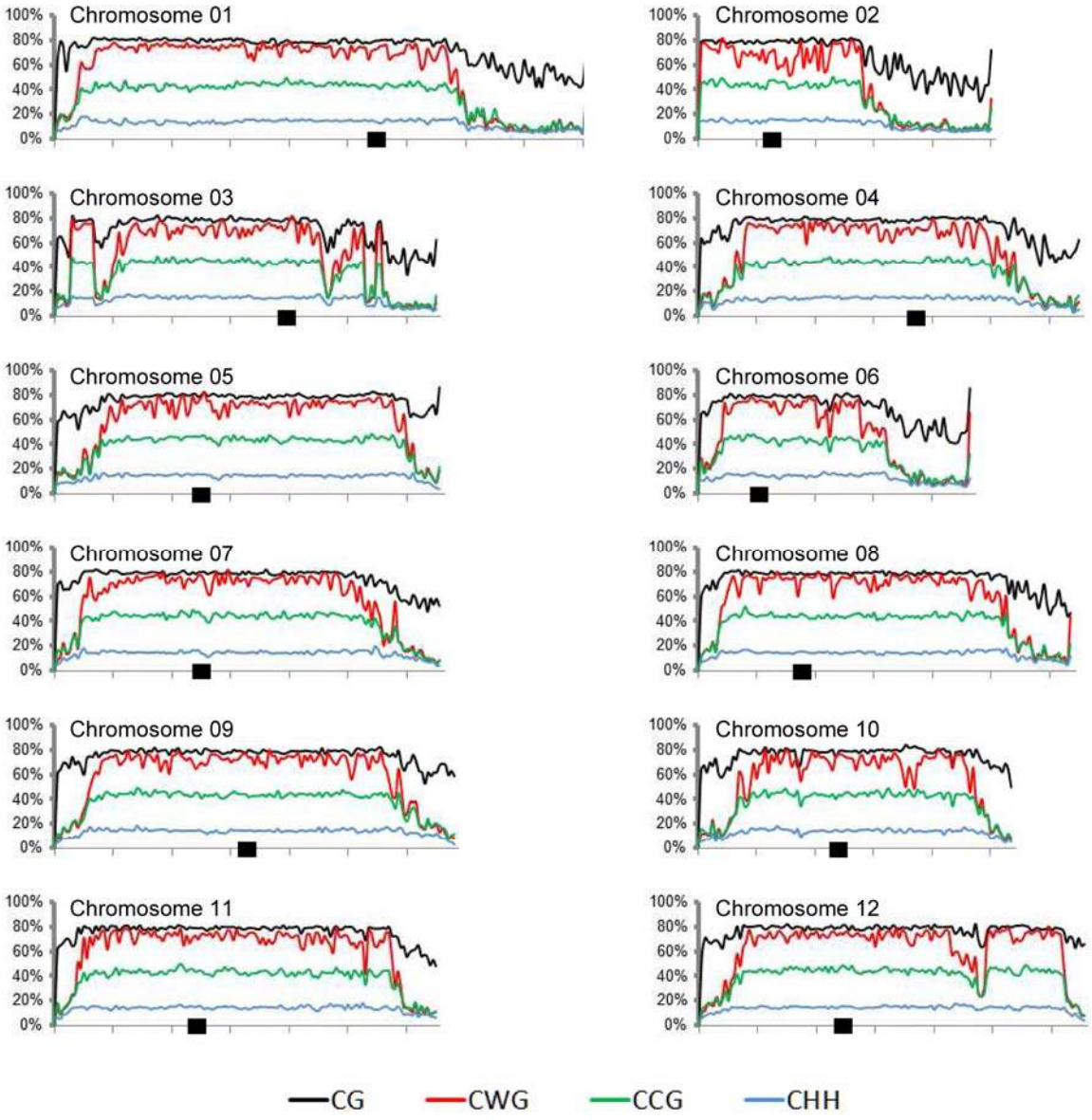

Supplementary Figure 2 | DNA cytosine methylation rates across the twelve tomato chomosomes of mature green fruit. Black rectangles indicate approximate centromere positions. Line colors reflect the indicated cytosine sequence contexts.

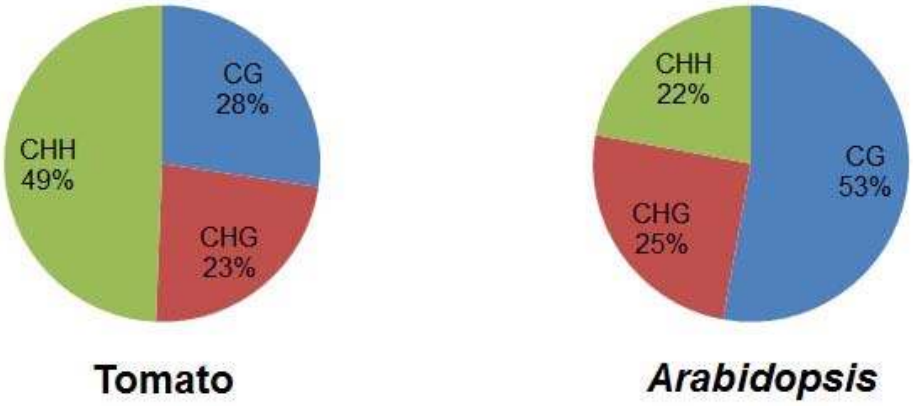

Supplementary Figure 3 | DNA cytosine methylation context in tomato and *Arabidopsis*. Fraction of 5-methylcytosines identified in each context for the tomato and *Arabidopsis* (Col-0) leaf tissues.

Nature Biotechnology: doi:10.1038/nbt.2462

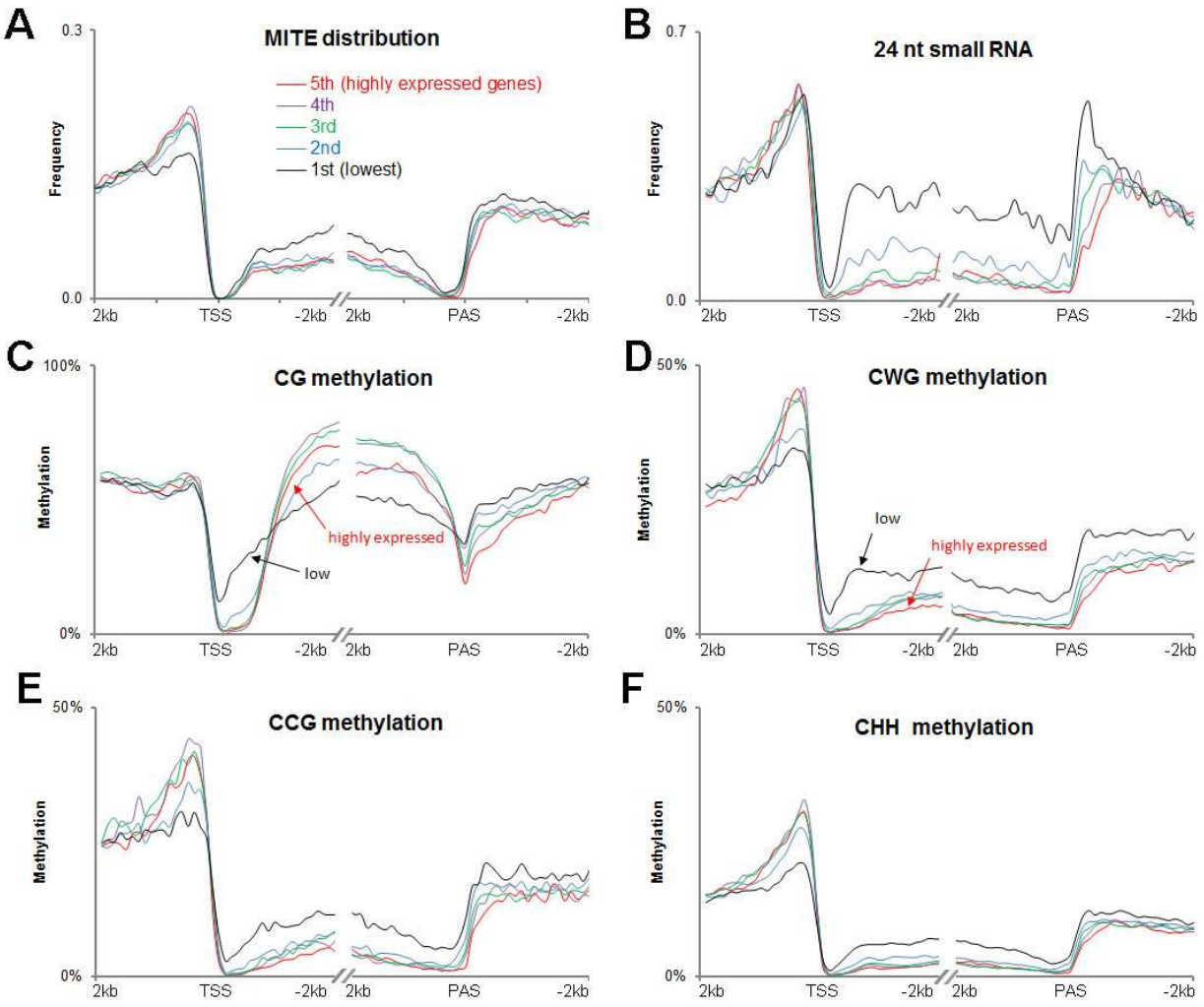

Supplementary Figure 4 | Association of DNA cytosine methylation, TE density, small RNA and gene expression. Genes were classified into 5 groups based on their expression level in tomato fruit at 39DPA (group 5: highest, group 1: lowest). (A) Distribution of miniature inverted transposable elements (MITEs) in the regions 2 kb upstream and downstream of TSS and PAS (bin size = 100 bp). (B) Distribution of 24nt small RNAs. (C) Distribution of CG methylation. (D) Distribution of CWG methylation. (E) Distribution of CCG methylation. (F) Distribution of CHH methylation. TSS: transcription start site; PAS: polyadenylation site.

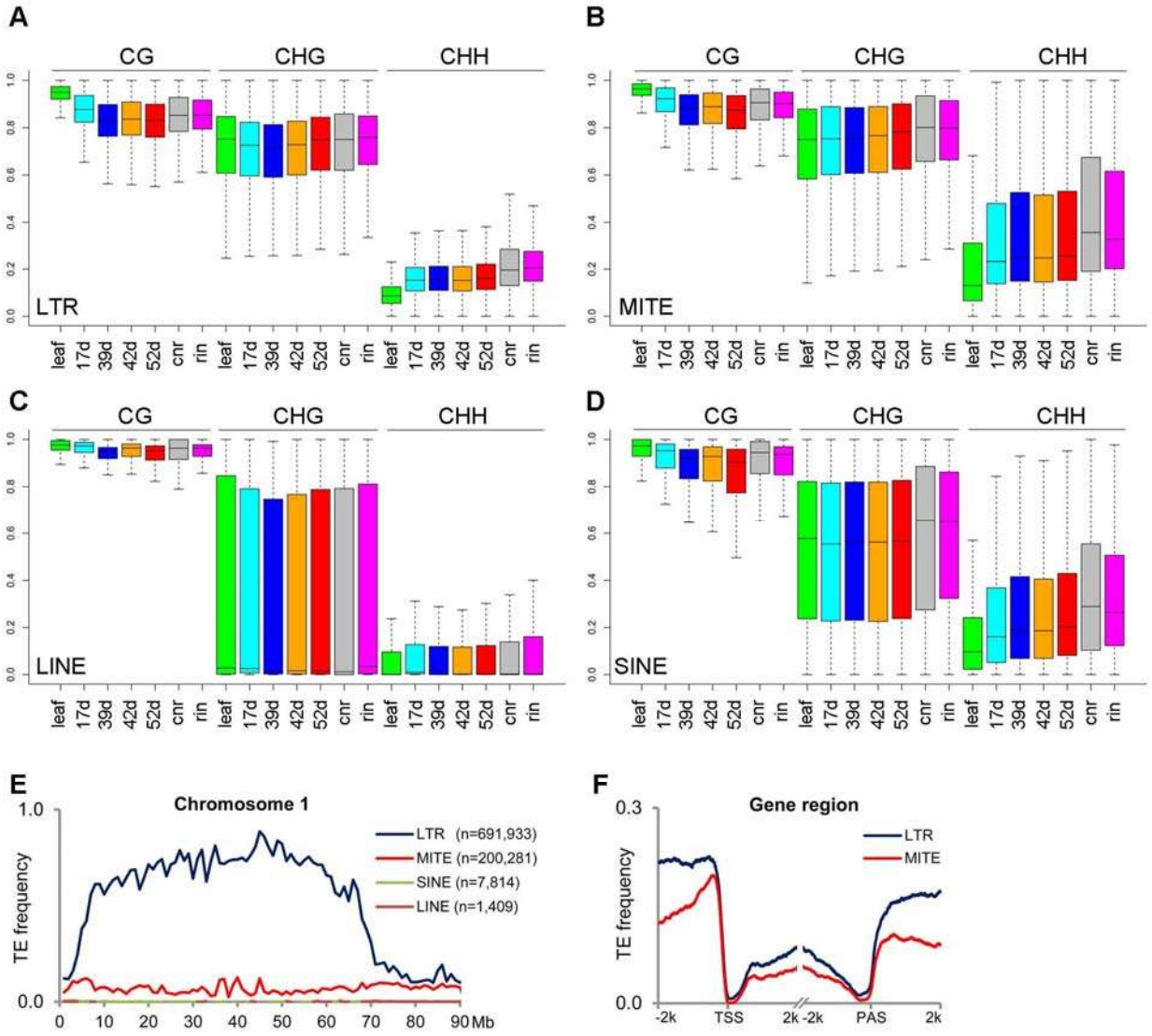

Supplementary Figure 5 | DNA cytosine methylation of transposable elements. (A) Methylation rate of long terminal repeats (LTRs). (B) Methylation rate of miniature inverted transposable elements (MITEs). (C) Methylation rate of long interspersed elements (LINEs). (D) Methylation rate of short interspersed elements (SINEs). (E) Distribution of different classes of TE in chromosome 1 and the total number of each class of annotated TEs in the tomato genome are shown (bin size = 500 kb). (F) Distribution of LTRs and MITEs in gene regions (bin size = 100 bp). TSS: transcription start site; PAS: polyadenylation site.

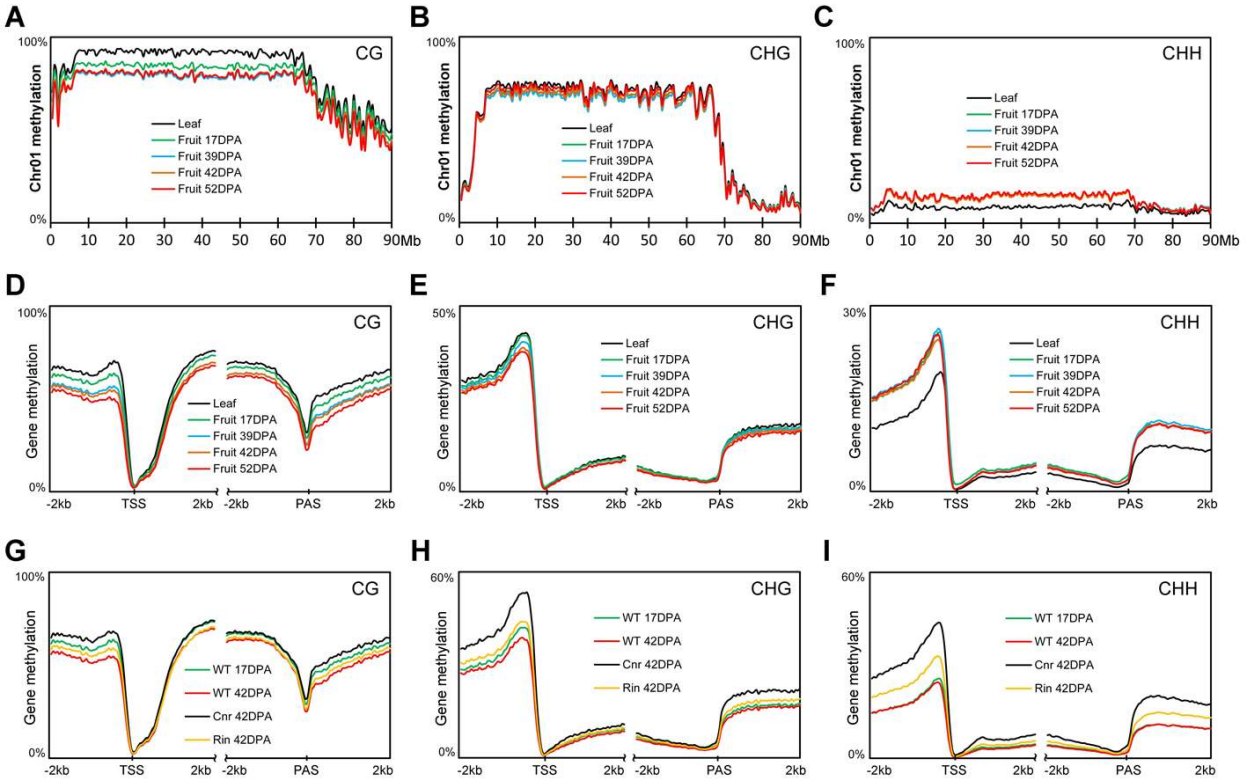

Supplementary Figure 6 | DNA cytosine methylation levels in chromosome 1 and genic regions. (A-C) Methylation rate of chromosome 1 in each sequence context (bin = 500 kb). (D-F) Methylation rate of gene bodies and surrounding regions (bin = 100 bp). (G-I) Methylation rate of non-ripening mutant *Cnr* and *rin* fruits at 42 DPA. TSS: transcription start site; PAS: polyadenylation site.

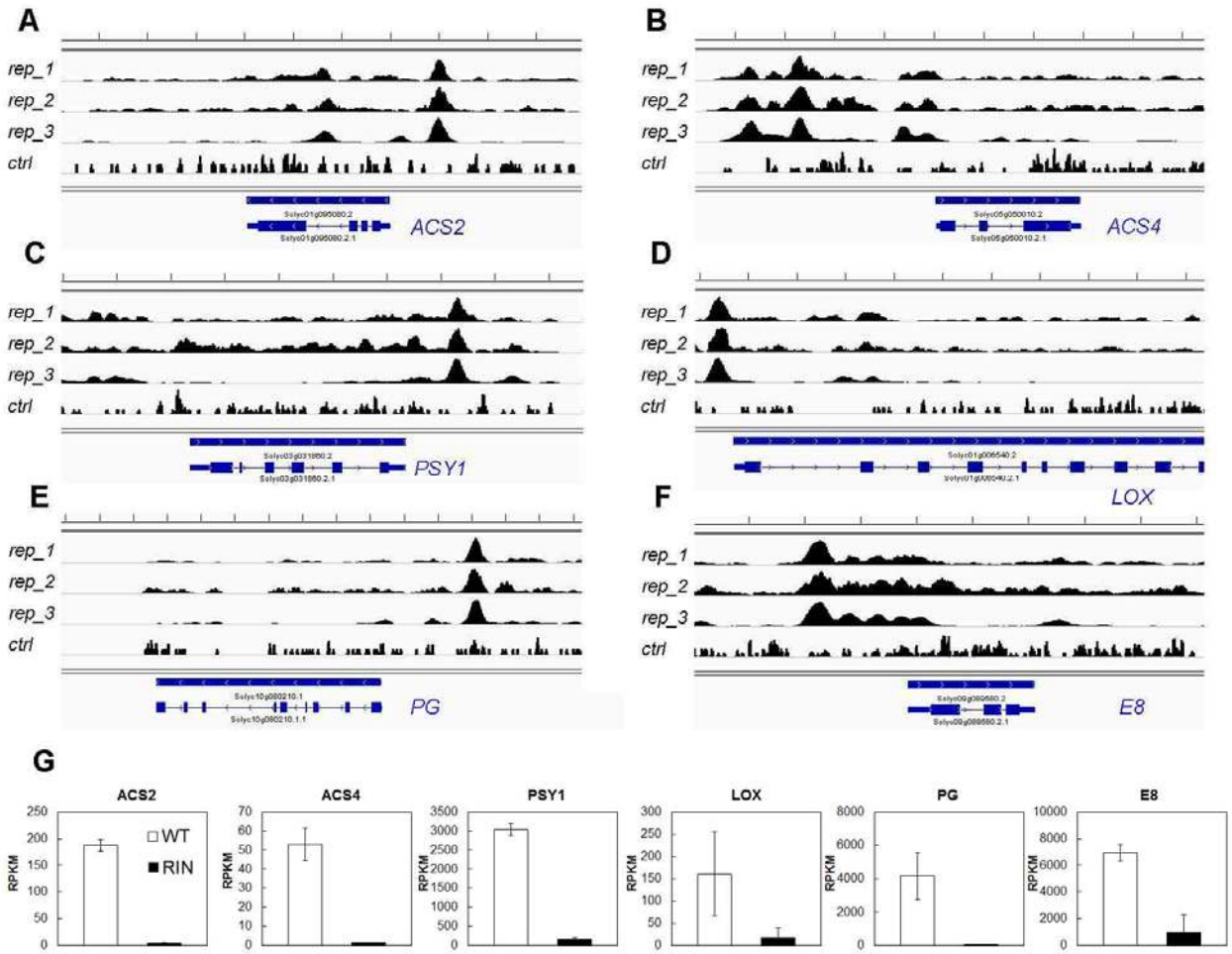

Supplementary Figure 7 | Targets of the MADS-box transcription factor RIN. Genome browser showing the ChIP-Seq peaks indicative of RIN binding in (A) *ACC SYNTHASE 2*, (B) *ACC SYNTHASE 4*, (C) *PHYTOENE SYNTHASE 1*, (D) *LIPOXYGENASES*, (E) *POLYGALACTURONASE* and (F) ethylene responsive gene *E8*. Three ChIP-Seq biological replicates (rep 1 to 3) and one negative control library are shown (Scale = 1 kb). (G) Ripening gene expression patterns in wild-type and *RIN* loss-of-function mutant.

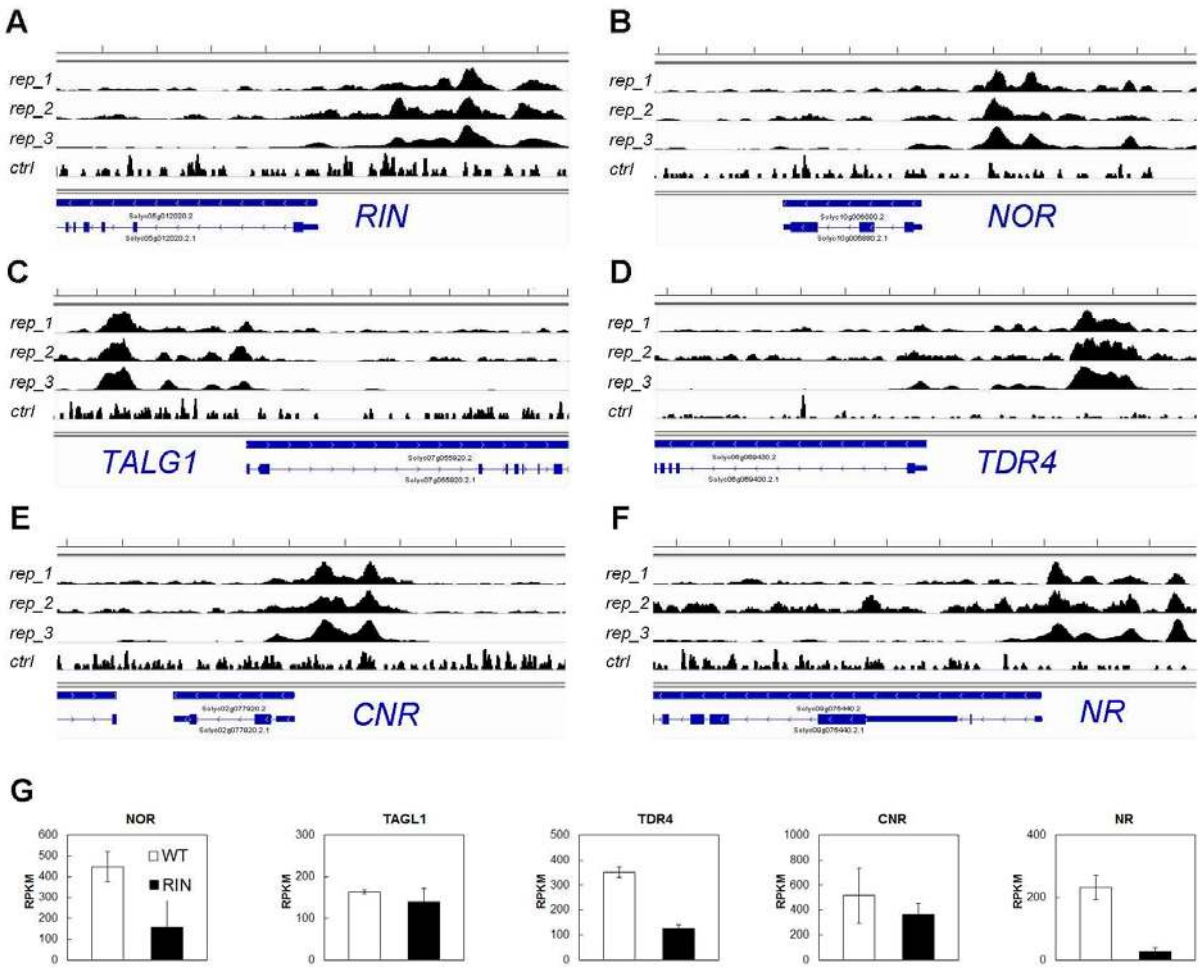

Supplementary Figure 8 | RIN targets known fruit ripening regulators and binds its own promoter. Genome browser showing the ChIP-Seq peaks indicative of RIN binding in (A) *RIN* itself, (B) NAC-domain transcription factor *NON-RIPENING* (*NOR*), (C) MADS-box transcription factor *TOMOATO AGAMOUS-LIKE 1* (*TAGL1*), (D) MADS-box transcription factor *TDR4*, (E) SPB transcription factor *COLORLESS NON-RIPENING* (*CNR*) and (F) ethylene receptor *NEVER-RIPE* (*NR*). Three ChIP-Seq biological replicates (rep 1 to 3) and one negative control library are shown (Scale = 1 kb). (G) Gene expression patterns in wild-type and *RIN* loss-of-function mutant.

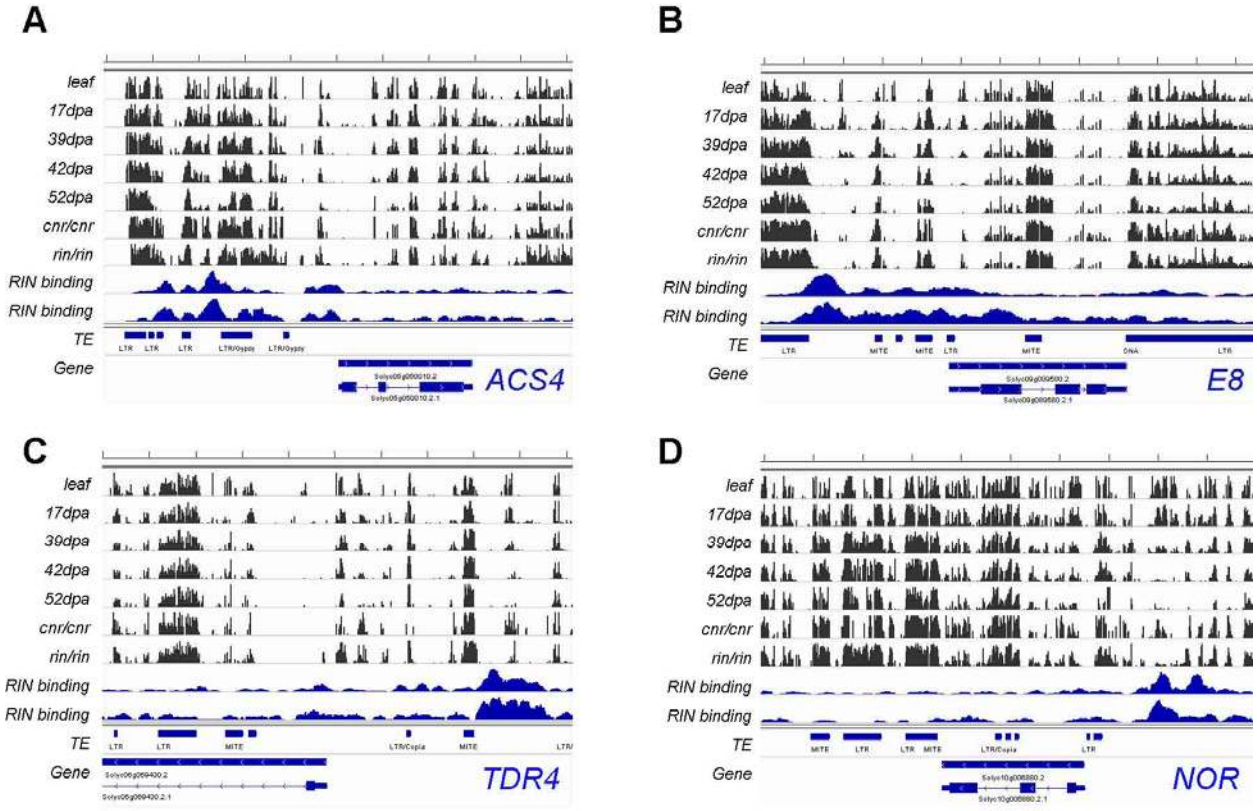

Supplementary Figure 9 | RIN binding sites and DMRs in fruit ripening regulatory gene loci. Genome browser showing cytosine methylation levels and ChIP-Seq peaks indicative of RIN binding in gene loci encoding (A) *ACC SYNTHASE 4* (*ACS4*), a rate limiting enzyme for ripening ethylene production, (B) fruit-specific ethylene responsive gene *E8*, (C) MADS-box transcription factor *TDR4* and (D) NAC domain containing transcription factor *NON-RIPENING* (*NOR*). Track labels from top to bottom: cytosine methylation levels in leaf, immature fruit (17dpa), mature green fruit (39dpa), ripening fruit (42dpa), ripened fruit (52dpa), *cnr* mutant fruit at 42dpa, *rin* mutant fruit at 42dpa, transposable elements (TEs), gene (scale = 1 kb).

Nature Biotechnology: doi:10.1038/nbt.2462

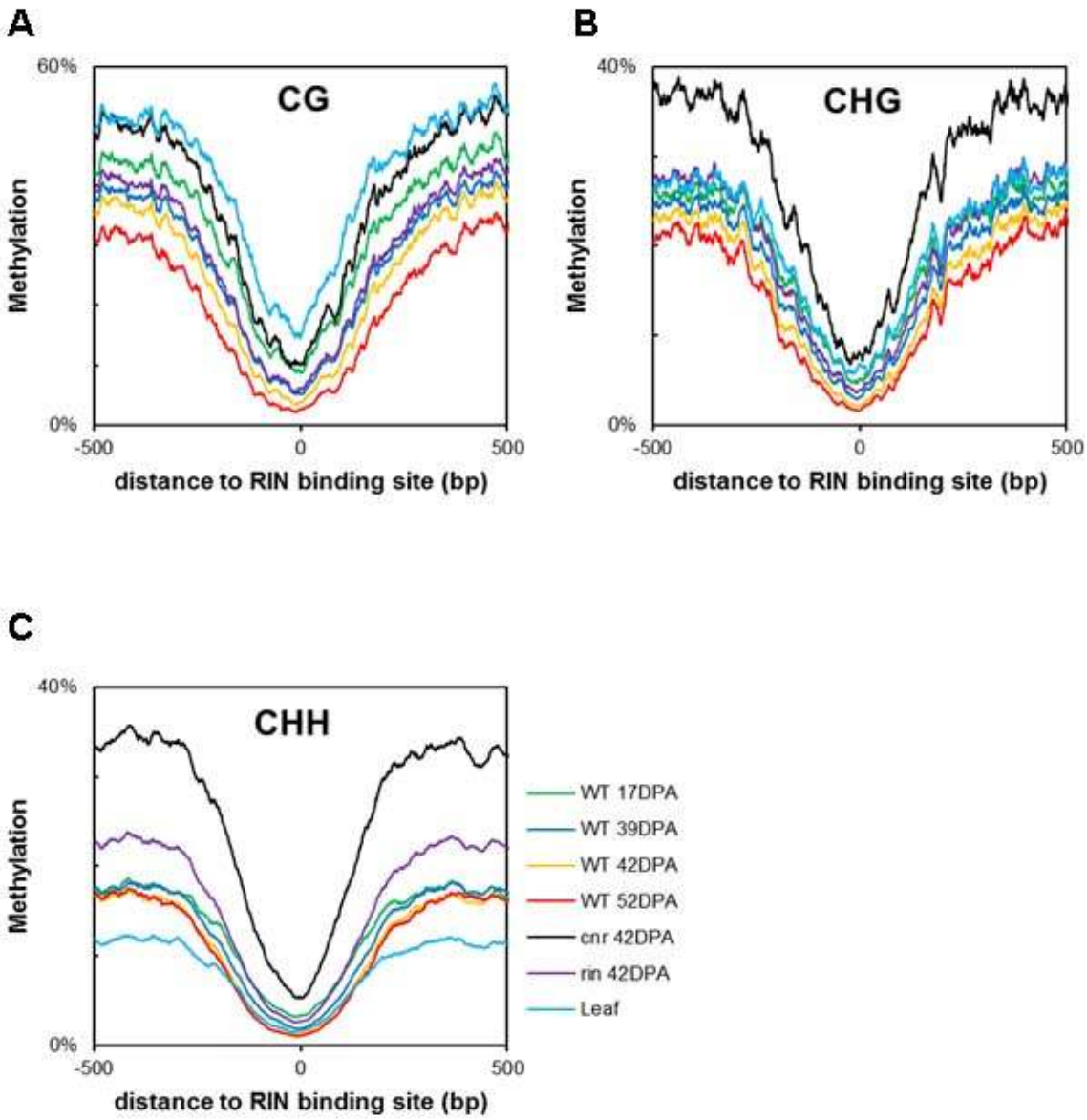

Supplementary Figure 10 | DNA cytosine methylation adjacent to RIN binding sites. (A-C) Average methylation levels near all RIN binding sites in each sequence context. The x-axis represents the distance to the RIN ChIP-Seq summit (bin = 20 bp).

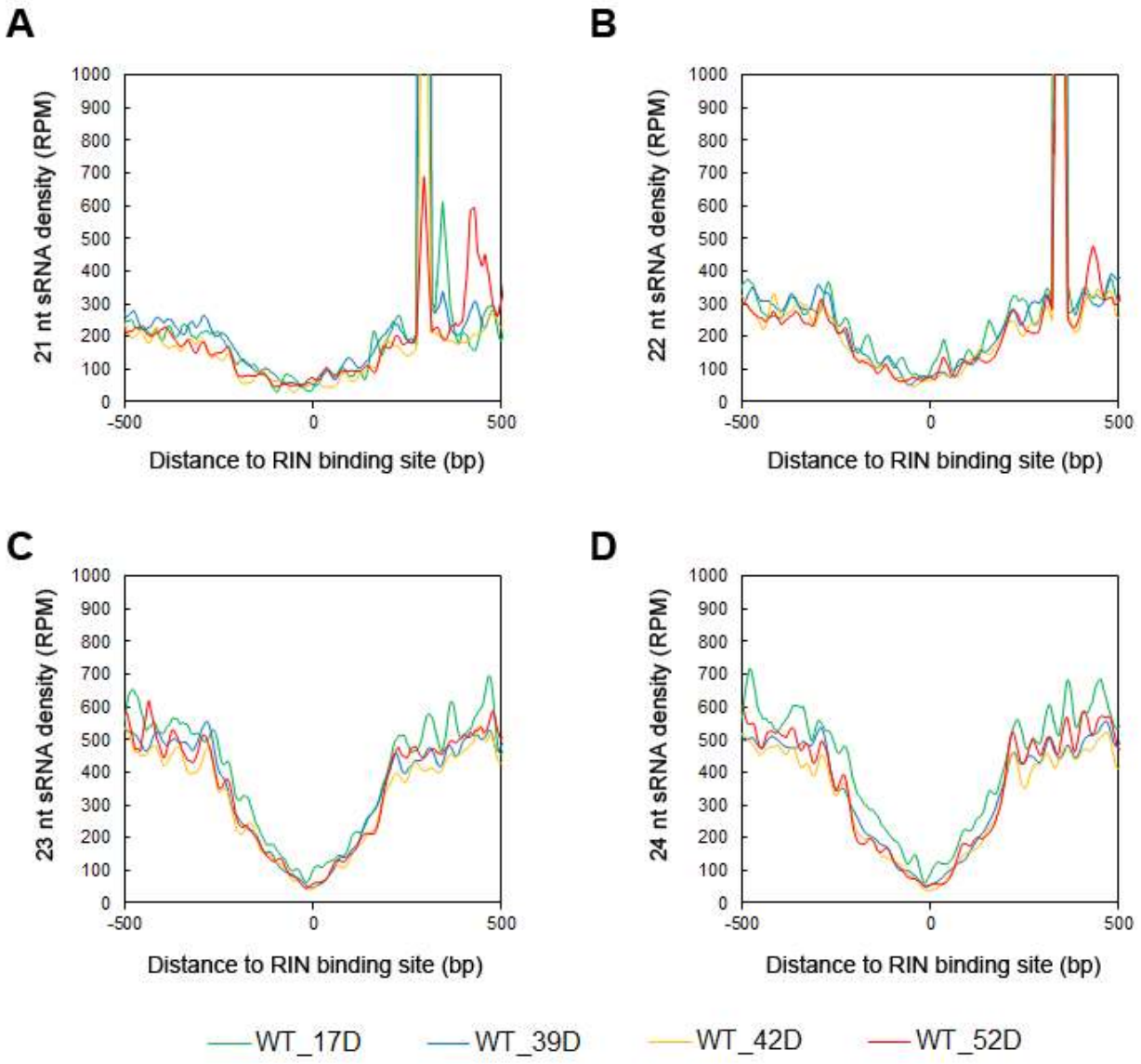

Supplementary Figure 11 | Small RNA density adjacent to RIN binding sites. The raw small RNA sequencing read counts near RIN binding sites were normalized by library size to read per million (RPM). The y-axis represent sRNA density, and x-axis represents the distance to the RIN ChIP-Seq summit (bin = 20 bp).